arXiv:0809.5226v2 [hep-th] 1 Oct 2008

On the problem of inflation in nonlinear multidimensional cosmological models

Tamerlan Saidov* and Alexander Zhuk†
Astronomical Observatory and Department of Theoretical Physics,
Odessa National University, 2 Dvoryanskaya St., Odessa 65082, Ukraine

We consider a multidimensional cosmological model with nonlinear quadratic R^2 and quartic R^4 actions. As a matter source, we include a monopole form field, D-dimensional bare cosmological constant and tensions of branes located in fixed points. In the spirit of the Universal Extra Dimensions models, the Standard Model fields are not localized on branes but can move in the bulk. We define conditions which ensure the stable compactification of the internal space in zero minimum of the effective potentials. Such effective potentials may have rather complicated form with a number of local minima, maxima and saddle points. Then, we investigate inflation in these models. It is shown that R^2 and R^4 models can have up to 10 and 22 e-foldings, respectively. These values are not sufficient to solve the homogeneity and isotropy problem but big enough to explain the recent CMB data. Additionally, R^4 model can provide conditions for eternal topological inflation. However, the main drawback of the given inflationary models consists in a value of spectral index n_s which is less than observable now $n_s \approx 1$. For example, in the case of R^4 model we find $n_s \approx 0.61$.

PACS numbers: 04.50.+h, 11.25.Mj, 98.80.-k

I. INTRODUCTION

Recently, very elegant idea of inflation has achieved spectacular success in explaining the acoustic peak structure seen in CMB (see e.g. [1]). It is very difficult to explain correctly the observable large-scale structure formation without taking into account the stage of early inflation. There is a big number of different models of inflation. However, the most of them are poorly related to fundamental physics. In these models, the stage of inflation occurs due to a special form of scalar field potential. Here, the origin of scalar field and the form of its potential is usually remained out of the scope of these papers. However, it is well known that scalar fields has naturel origin from higher-dimensional theories. They are geometrical moduli (radions, gravexcitons) which are related to the shape of internal spaces (to scale factors of the internal spaces). After dimensional reduction to four dimensions, scalar field potential is completely defined by the topology and matter content of original higher-dimensional model [2, 3]. Thus, it is of undoubted interest to realize inflation in these models (see e.g. [4, 5, 6] in string theory and [7] in multidimensional cosmological models and references therein).

On the other hand, scalar fields with corresponding potentials originate naturally from nonlinear gravitational models where Lagrangian is a function of scalar curvature $f(R)$. It is well known that such models are equivalent to linear ones plus scalar field. This scalar field corresponds to an additional degree of freedom of nonlinear models. For motivation of these theories, see review [8]. For example, among others higher-order gravity theories, $f(R)$ theories are free of ghosts and of Ostrogradski instability [9]. These models attract great attention because can provide the late-time acceleration of our Universe due to a special form of scalar field potentials (see e.g. [8, 10, 11] and references therein), which is interesting alternative to the cosmological constant. These models can also provide the stage of early inflation both in four-dimensional (see the pioneering paper by Starobinsky [12] and numerous references in [8, 10]) and multidimensional [11, 13, 14] cases.

In our paper we combine both of these approaches. Namely, we consider multidimensional models with nonlinear action. To start with, we investigate the most simple linear multidimensional model. We show that such model can provide power-law inflation. Unfortunately, it takes place for the branch where internal space is decompactified [1]. Then, to get inflation of the external space with subsequent stabilization of the internal spaces, we turn to multidimensional nonlinear models with quadratic and quartic nonlinearities. First, we obtain the conditions of the internal space compactification (stabilization). Second, for corresponding effective potentials, we investigate the possibility of the external space inflation. We show that in the quadratic and quartic models we can achieve 10 and 22 e-folds, respectively. These numbers are sufficient to explain the present day CMB date, but not enough to solve the horizon and flatness problems. However, 22 e-foldings is rather big number to encourage the following investigation of the nonlinear multidimensional models to find theories where this number will approach to 50-60 e-folds. Even more, this number (50-60) can be reduced in

*Electronic address: tamerlan-saidov@yandex.ru
†Electronic address: zhuk@paco.net

[1] Each time when we consider multidimensional cosmological models we should remember about the problem of the internal space stabilization/compactification. If such stabilization is absent we confront with the variation of four-dimensional fundamental constants. General method of the internal space stabilization was described in [3] and was applied after that to numerous models. In the present paper, we follow also this method.

models with long matter dominated stage followed by inflation with subsequent decay into radiation. Precisely this scenario takes place for our models where we find that e-folds can be reduced by 6 if the mass of decaying scalar field $m \sim 1$TeV. So, we believe that the number of e-folds is not a big problem for proposed models. The main problem consists in spectral index $n_s \approx 0.61$ (for the quartic model) which is less than observable $n_s \approx 1$. A possible solution of this problem may consist in more general form of the nonlinearity $f(R)$. For example, it was observed in [15] that simultaneous consideration quadratic and quartic nonlinearities can flatten the effective potential. We postpone the investigation of this problem for our following paper.

To conclude, we want to indicate two interesting features of models under consideration. First, the quartic model can provide the topological inflation. Here, due to quantum fluctuation of scalar fields, inflating domain wall has fractal structure (inflating domain wall will contain a number of new inflating domain walls and each such domain walls will contain again a new inflating walls etc [16]). So, we arrive at the eternal inflation. Second, obtained solution has the property of the self-similarity transformation (see Appendix B). It means that in the case of zero minimum of the effective potential and fixed positions for extrema in $(\varphi, \phi)-$plane, the change of the hight of extrema results in rescaling of the dynamical characteristics of the model (graphics of the number of e-folds, scalar fields, the Hubble parameter and the acceleration parameter versus synchronous time) along the time axis. The decrease (increase) of hight in c times (c is a constant) leads to the stretch (shrink) of these figures along the time axis in $\sqrt{c}$ times.

The paper is structured as follows. In Sec. II we consider the linear (on scalar curvature) model. The nonlinear quadratic R^2 and quartic R^4 models are investigated in Sec. III and Sec. IY, respectively. Here, we find the range of parameters where the internal space is stabilized and investigate a possibility for the external space inflation. A brief discussion of the obtained results is presented in the concluding Sec. Y. The Friedmann equations for multi-component scalar field models are reduced to the system of dimensionless first order ODEs in Appendix A. In Appendix B, we show that the dynamical characteristics (e.g. the Hubble parameter, the acceleration parameter) of considered nonlinear models satisfy the self-similarity condition.

II. LINEAR MODEL

To start with, let us define the topology of our models. We consider a factorizable D-dimensional metric

$$g^{(D)} = g^{(0)}(x) + L_{Pl}^2 e^{2\beta^1(x)} g^{(1)}\,, \qquad (2.1)$$

which is defined on a warped product manifold $M = M_0 \times M_1$. M_0 describes external D_0-dimensional space-time (usually, we have in mind that $D_0 = 4$) and M_1 corresponds to d_1-dimensional internal space which is a flat orbifold[2] with branes in fixed points. Scale factor of the internal space depends on coordinates x of the external space-time: $a_1(x) = L_{Pl} e^{\beta^1(x)}$, where L_{Pl} is the Planck length.

First, we consider the linear model $f(R) = R$ with D-dimensional action of the form

$$S = \frac{1}{2\kappa_D^2}\int_M d^D x \sqrt{|g^{(D)}|}\left\{R[g^{(D)}] - 2\Lambda_D\right\} + S_m + S_b\,. \qquad (2.2)$$

Λ_D is a bare cosmological constant[3]. In the spirit of Universal Extra Dimension models [17], the Standard Model fields are not localized on the branes but can move in the bulk. The compactification of the extra dimensions on orbifolds has a number of very interesting and useful properties, e.g. breaking (super)symmetry and obtaining chiral fermions in four dimensions (see e.g. paper by H.-C. Cheng at al in [17]). The latter property gives a possibility to avoid famous no-go theorem of KK models (see e.g. [18]). Additional arguments in favor of UED models are listed in [19].

Following a generalized Freund-Rubin ansatz [20] to achieve a spontaneous compactification $M \to \bar{M} = M_0 \times M_1$, we endow the extra dimensions with real-valued solitonic form field $F^{(1)}$ with an action:

$$S_m = -\frac{1}{2}\int_M d^D x \sqrt{|g^{(D)}|}\frac{1}{d_1!}\left(F^{(1)}\right)^2\,, \qquad (2.3)$$

This form field is nested in d_1-dimensional factor space M_1, i.e. $F^{(1)}$ is proportional to the world-volume of the internal space. In this case $(1/d_1!)\left(F^{(1)}\right)^2 = \bar{f}_1^2/a_1^{2d_1}$, where $\bar{f}_1$ is a constant of integration [21].

Branes in fixed points contribute in action functional (2.2) in the form [22]:

$$S_b = \sum_{\substack{fixed\\points}}\int_{M_0} d^4 x \sqrt{|g^{(0)}(x)|}\; L_b\Big|_{\substack{fixed\\point}}\,, \qquad (2.4)$$

where $g^{(0)}(x)$ is induced metric (which for our geometry (2.1) coincides with the metric of the external space-time in the Brans-Dicke frame) and L_b is the matter Lagrangian on the brane. In what follows, we consider the case where branes are only characterized by their tensions $L_{b(k)} = -\tau_{(k)}$, $k = 1, 2, \ldots, m$ and m is the number of branes.

---

[2] For example, S^1/Z_2 and T^2/Z_2 which represent circle and square folded onto themselves due to Z_2 symmetry.

[3] Such cosmological constant can originate from D-dimensional form field which is proportional to the D-dimensional world-volume: $F^{MN\ldots Q} = (C/\sqrt{|g^{(D)}|})\epsilon^{MN\ldots Q}$. In this case the equations of motion gives $C = const$ and F^2 term in action is reduced to $(1/D!)F_{MN\ldots Q}F^{MN\ldots Q} = -C^2$.

Let β_0^1 be the internal space scale factor at the present time and $\bar{\beta}^1 = \beta^1 - \beta_0^1$ describes fluctuations around this value. Then, after dimensional reduction of the action (2.1) and conformal transformation to the Einstein frame $g^{(0)}_{\mu\nu} = \left(e^{d_1\bar{\beta}^1}\right)^{-2/(D_0-2)} \tilde{g}^{(0)}_{\mu\nu}$, we arrive at effective D_0-dimensional action of the form

$$S_{eff} = \frac{1}{2\kappa_0^2}\int_{M_0} d^{D_0}x\sqrt{|\tilde{g}^{(0)}|}\left\{R[\tilde{g}^{(0)}] - \tilde{g}^{(0)\mu\nu}\partial_\mu\varphi\partial_\nu\varphi - 2U_{eff}(\varphi)\right\}, \quad (2.5)$$

where scalar field φ is defined by the fluctuations of the internal space scale factor:

$$\varphi \equiv \sqrt{\frac{d_1(D-2)}{D_0-2}}\,\bar{\beta}^1 \quad (2.6)$$

and $G := \kappa_0^2/8\pi := \kappa_D^2/(8\pi V_{d_1})$ (V_{d_1} is the internal space volume at the present time) denotes the D_0-dimensional gravitational constant. The effective potential $U_{eff}(\varphi)$ reads (hereafter we put $D_0 = 4$):

$$U_{eff}(\varphi) = e^{-\sqrt{\frac{2d_1}{d_1+2}}\,\varphi}\left[\Lambda_D + f_1^2 e^{-2\sqrt{\frac{2d_1}{d_1+2}}\,\varphi} - \lambda e^{-\sqrt{\frac{2d_1}{d_1+2}}\,\varphi}\right], \quad (2.7)$$

where $f_1^2 \equiv \kappa_D^2\bar{f}_1^2/a_{(0)1}^{2d_1}$ and $\lambda \equiv -\kappa_0^2\sum_{k=1}^m \tau_{(k)}$.

Now, we should investigate this potential from the point of the external space inflation and the internal space stabilization. First, we consider the latter problem. It is clear that internal space is stabilized if $U_{eff}(\varphi)$ has a minimum with respect to φ. The position of minimum should correspond to the present day value $\varphi = 0$. Additionally, we can demand that the value of the effective potential in the minimum position is equal to the present day dark energy value $U_{eff}(\varphi = 0) \sim \Lambda_{DE} \sim 10^{-57}\mathrm{cm}^{-2}$. However, it results in very flat minimum of the effective potential which in fact destabilizes the internal space [22]. To avoid this problem, we shall consider the case of zero minimum $U_{eff}(\varphi = 0) = 0$.

The extremum condition $dU_{eff}/d\varphi|_{\varphi=0} = 0$ and zero minimum condition $U_{eff}(\varphi = 0) = 0$ result in a system of equations for parameters Λ_D, f_1^2 and λ which has the following solution:

$$\Lambda_D = f_1^2 = \lambda/2\,. \quad (2.8)$$

For the mass of scalar field excitations (gravexcitons/radions) we obtain: $m^2 = d^2U_{eff}/d\varphi^2\big|_{\varphi=0} = (4d_1/(d_1+2))\Lambda_D$. In Fig. 1 we present the effective potential (2.7) in the case $d_1 = 3$ and $\Lambda_D = 10$. It is worth of noting that usually scalar fields in the present paper are dimensionless[4] and $U_{eff}, \Lambda_D, f_1^2, \lambda$ are measured in M_{Pl}^2 units.

Let us turn now to the problem of the external space inflation. As far as the external space corresponds to our Universe, we take metric $\tilde{g}^{(0)}$ in the spatially flat Friedmann-Robertson-Walker form with scale factor $a(t)$. Scalar field φ depends also only on the synchronous/cosmic time t (in the Einstein frame).

It can be easily seen that for $\varphi >> 0$ (more precisely, for $\varphi > \varphi_{max} = \sqrt{(d_1+2)/2d_1}\ln 3$) the potential (2.7) behaves as

$$U_{eff}(\varphi) \approx \Lambda_D e^{-\sqrt{q}\,\varphi}\,, \quad (2.9)$$

with

$$q := \frac{2d_1}{d_1+2}\,. \quad (2.10)$$

It is well known (see e.g. [23, 24, 25, 26]) that for such exponential potential scale factor has the following asymptotic form:

$$a(t) \sim t^{2/q}\,. \quad (2.11)$$

Thus, the Universe undergoes the power-law inflation if $q < 2$. Precisely this condition holds for eq. (2.10) if $d_1 \geq 1$.

It can be easily verified that $\varphi > \varphi_{max}$ is the only region of the effective potential where inflation takes place. Indeed, in the region $\varphi < 0$ the leading exponents are too large, i.e. the potential is too steep. The local maximum of the effective potential $U_{eff}|_{max} = (4/27)\Lambda_D$ at $\varphi_{max} = \sqrt{(d_1+2)/2d_1}\ln 3$ is also too steep for inflation because the slow-roll parameter $\eta_{max} = \frac{1}{U_{eff}}\frac{d^2U_{eff}}{d\varphi^2}\Big|_{max} = -\frac{3d_1}{d_1+2} \Rightarrow 1 \leq |\eta_{max}| < 3$ and does not satisfy the inflation condition $|\eta| < 1$. Topological inflation is also absent here because the distance between global minimum and local maximum $\varphi_{max} = \sqrt{(d_1+2)/2d_1}\ln 3 \leq 1.35$ is less than critical value $\varphi_{cr} \geq 1.65$ (see [15, 27, 28]). It is worth of noting that η_{max} and φ_{max} depend only on the number of dimensions d_1 of the internal space and do not depend on the hight of the local maximum (which is proportional to Λ_D).

Therefore, we have two distinctive regions in this model. In the first region, at the left of the maximum in the vicinity of the minimum, scalar field undergoes the damped oscillations. These oscillations have the form of massive scalar fields in our Universe (in [3] these excitations were called gravitational excitons and later (see e.g. [29]) these geometrical moduli oscillations were also named radions). Their lifetime with respect to the decay $\varphi \to 2\gamma$ into radiation is [30, 31, 32] $\tau \sim (M_{Pl}/m)^3 T_{Pl}$. For example,

[4] To restore dimension of scalar fields we should multiply their dimensionless values by $M_{Pl}/\sqrt{8\pi}$.

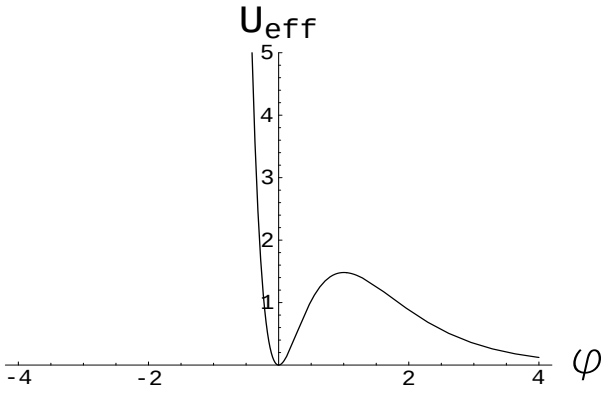

FIG. 1: The form of the effective potential (2.7) in the case $d_1 = 3$ and $\Lambda_D = f_1^2 = \lambda/2 = 10$.

we obtain $\tau \sim 10\,\mathrm{s}, 10^{-2}\,\mathrm{s}$ for $m \sim 10\,\mathrm{TeV}, 10^2\,\mathrm{TeV}$ correspondingly. We remind that in our case $m^2 = (4d_1/(d_1+2))\Lambda_D$. Therefore, this is the graceful exit region. Here, the internal space scale factor, after decay its oscillations into radiation, is stabilized at the present day value and the effective potential vanishes due to zero minimum. In second region, at the right of the maximum of the potential, our Universe undergoes the power-low inflation. However, it is impossible to transit from the region of inflation to the graceful exit region because given inflationary solution satisfies the following condition $\dot{\varphi} > 0$. There is also serious additional problem connected with obtained inflationary solution. The point is that for the exponential potential of the form (2.9), the spectral index reads [23, 25][5]:

$$n_s = \frac{2-3q}{2-q}\,. \tag{2.12}$$

In our case (2.10), it results in $n_s = 1 - d_1$. Obviously, for $d_1 \geq 1$ this value is very far from observable data $n_s \approx 1$. Therefore, it is necessary to generalize our linear model.

III. NONLINEAR QUADRATIC MODEL

As follows from the previous section, we want to generalize the effective potential making it more complicated and having more reach structure. Introduction of an additional minimal scalar field ϕ is one of possible ways. We can do it "by hand", inserting minimal scalar field ϕ with a potential $U(\phi)$ in linear action (2.2)[6]. Then, effective potential takes the form

$$\begin{aligned} U_{eff}(\varphi,\phi) &= e^{-\sqrt{\frac{2d_1}{d_1+2}}\,\varphi}\Big[U(\phi) + f_1^2 e^{-2\sqrt{\frac{2d_1}{d_1+2}}\,\varphi} \\ &- \lambda e^{-\sqrt{\frac{2d_1}{d_1+2}}\,\varphi}\Big]\,, \end{aligned} \tag{3.1}$$

where we put $\Lambda_D = 0$ in (2.2).

However, it is well known that scalar field ϕ can naturally originate from the nonlinearity of higher-dimensional models where the Hilbert-Einstein linear lagrangian R is replaced by nonlinear one $f(R)$. These nonlinear theories are equivalent to the linear ones with a minimal scalar field (which represents additional degree of freedom of the original nonlinear theory). It is not difficult to verify (see e.g. [13, 21]) that nonlinear model

$$\begin{aligned} S &= \frac{1}{2\kappa_D^2}\int_M d^D x\sqrt{|\overline{g}^{(D)}|}f(\overline{R}) \\ &- \frac{1}{2}\int_M d^D x\sqrt{|g^{(D)}|}\frac{1}{d_1!}\left(F^{(1)}\right)^2 \\ &- \sum_{k=1}^{m}\int_{M_0} d^4x\sqrt{|g^{(0)}(x)|}\;\tau_{(k)} \end{aligned} \tag{3.2}$$

is equivalent to a linear one with conformally related metric

$$g_{ab}^{(D)} = e^{2A\phi/(D-2)}\overline{g}_{ab}^{(D)} \tag{3.3}$$

plus minimal scalar field $\phi = \ln[df/d\overline{R}]/A$ with a potential

$$U(\phi) = \frac{1}{2}e^{-B\phi}\left[\overline{R}(\phi)e^{A\phi} - f(\overline{R}(\phi))\right]\,, \tag{3.4}$$

[5] With respect to conformal time, solution (2.11) reads $a(\eta) \sim \eta^{1+\beta}$ where $\beta = -(4-q)/(2-q)$. It was shown in [33] that for such inflationary solution (with $q < 2$) the spectral index of density perturbation is given by $n_s = 2\beta + 5$ resulting again in (2.12).

[6] If such scalar field is the only matter field in these models, it is known (see e.g. [7, 13]) that the effective potential can has only negative minimum. i.e. the models are asymptotical AdS. To uplift this minimum to nonnegative values, it is necessary to add form-fields [21].

where $A = \sqrt{(D-2)/(D-1)} = \sqrt{(d_1+2)/d_1+3}$ and $B = D/\sqrt{(D-2)(D-1)} = A(d_1+4)/(d_1+2)$. After dimensional reduction of this linear model, we obtain an effective D_0-dimensional action of the form

$$S_{eff} = \frac{1}{2\kappa_0^2}\int_{M_0} d^{D_0}x\sqrt{|\tilde{g}^{(0)}|}\left[R[\tilde{g}^{(0)}] - \tilde{g}^{(0)\mu\nu}\partial_\mu\varphi\partial_\nu\varphi - \tilde{g}^{(0)\mu\nu}\partial_\mu\phi\partial_\nu\phi - 2U_{eff}(\varphi,\phi)\right], \quad (3.5)$$

with effective potential exactly of the form (3.1). It is worth to note that we suppose that matter fields are coupled to the metric $g^{(D)}$ of the linear theory (see also analogous approach in [34]). Because in all considered below models both fields φ and ϕ are stabilized in the minimum of the effective potential, such convention results in a simple redefinition/rescaling of the matter fields and effective four-dimensional fundamental constants. After such stabilization, the Einstein and Brans-Dicke frames are equivalent each other (metrics $g^{(0)}$ and $\tilde{g}^{(0)}$ coincide with each other), and linear $g^{(D)}$ and nonlinear $\overline{g}^{(D)}$ metrics in (3.3) are related via constant prefactor (models became asymptotically linear)[7].

Let us consider first the **quadratic theory**

$$f(\bar{R}) = \bar{R} + \xi\bar{R}^2 - 2\Lambda_D\,. \quad (3.6)$$

For this model the scalar field potential (3.4) reads:

$$U(\phi) = \frac{1}{2}e^{-B\phi}\left[\frac{1}{4\xi}\left(e^{A\phi}-1\right)^2 + 2\Lambda_D\right]. \quad (3.7)$$

It was proven [7] that the internal space is stabilized if the effective potential (3.1) has a minimum with respect to both fields φ and ϕ. It can be easily seen from the form of $U_{eff}(\varphi,\phi)$ that minimum ϕ_0 of the potential $U(\phi)$ coincides with the minimum of $U_{eff}(\varphi,\phi)$: $dU/d\phi|_{\phi_0} = 0 \to \partial_\phi U_{eff}|_{\phi_0} = 0$. For minimum $U(\phi_0)$ we obtain [13]:

$$U(\phi_0) = \frac{1}{8\xi}x_0^{\frac{-D}{D-2}}\left[(x_0-1)^2 + 8\xi\Lambda_D\right], \quad (3.8)$$

where we denote the constant $x_0 := \exp(A\phi_0) = \left(A - B + \sqrt{A^2 + (2A-B)B\,8\xi\Lambda_D}\right)/(2A-B)$. It is the global minimum and the only extremum of $U(\phi)$. Nonnegative minimum of the effective potential U_{eff} takes place for positive $\xi, \Lambda_D > 0$. If $\xi, \Lambda_D > 0$, the potential $U(\phi)$ has asymptotic behavior $U(\phi) \to +\infty$ for $\phi \to \pm\infty$.

The relations (2.8), where we should make the substitution $\Lambda_D \to U(\phi_0)$, are the necessary and sufficient conditions of the zero minimum of the effective potential $U_{eff}(\varphi,\phi)$ at the point $(\varphi = 0, \phi = \phi_0)$. Thus, if parameters of the quadratic models satisfy the conditions $U(\phi_0) = f_1^2 = \lambda/2$, we arrive at zero global minimum: $U_{eff}(0,\phi_0) = 0$.

It is clear that profile $\phi = \phi_0$ of the effective potential U_{eff} has a local maximum in the region $\varphi > 0$ because $U_{eff}(\varphi, \phi = \phi_0) \to 0$ if $\varphi \to +\infty$. Such profile has the form shown in Fig.1. Thus, the effective potential U_{eff} has a saddle point $(\varphi = \varphi_{max}, \phi = \phi_0)$ where $\varphi_{max} = \sqrt{(d_1+2)/2d_1}\ln 3$. At this point $U_{eff}|_{max} = (4/27)U(\phi_0)$. The Figure 2 demonstrates the typical contour plot of the effective potential (3.1) with the potential $U(\phi)$ of the form (3.7) in the vicinity of the global minimum and the saddle point.

Let us discuss now a possibility of the external space inflation in this model. It can be easily realized that for all models of the form (3.1) in the case of local zero minimum at $(\varphi = 0, \phi_0)$, the effective potential will also have a saddle point at $(\varphi = \varphi_{max}, \phi_0)$ with $\varphi_{max} = \sqrt{(d_1+2)/2d_1}\ln 3 < \varphi_{cr} = 1.65$ and the slow-roll parameter $|\eta_\varphi|$ in this point cannot be less than 1: $|\eta_\varphi| = 3d_1/(d_1+2) \geq 1$. Therefore, such saddles are too steep (in the section $\phi = \phi_0$) for the slow-roll and topological inflations However, as we shall see below, a short period of De Sitter-like inflation is possible if we start not precisely at the saddle point but first move in the vicinity of the saddle along the line $\varphi \approx \varphi_{max}$ with subsequent turn into zero minimum along the line $\phi \approx \phi_0$. Similar situation happens for trajectories from different regions of the effective potential which can reach this saddle and spend here a some time (moving along the line $\varphi \approx \varphi_{max}$).

Let us consider now regions where the following conditions take place:

$$U(\phi) \gg f_1^2 e^{-2\sqrt{\frac{2d_1}{d_1+2}}\,\varphi}\,, \quad \lambda e^{-\sqrt{\frac{2d_1}{d_1+2}}\,\varphi}. \quad (3.9)$$

For the potential (3.7) these regions exist both for negative and positive ϕ. In the case of positive ϕ with $\exp(A\phi) \gg \max\left\{1\,, (8\xi\Lambda_D)^{1/2}\right\}$ we obtain

$$U_{eff} \approx \frac{1}{8\xi}e^{-\sqrt{q}\,\varphi}e^{\sqrt{q_1}\,\phi}\,, \quad (3.10)$$

where q is defined by Eq. (2.10), $q_1 := (2A-B)^2 = d_1^2/[(d_1+2)(d_1+3)]$ and $q > q_1$. For potential (3.10)

[7] However, small quantum fluctuations around the minimum of the effective potential distinguish these metrics.

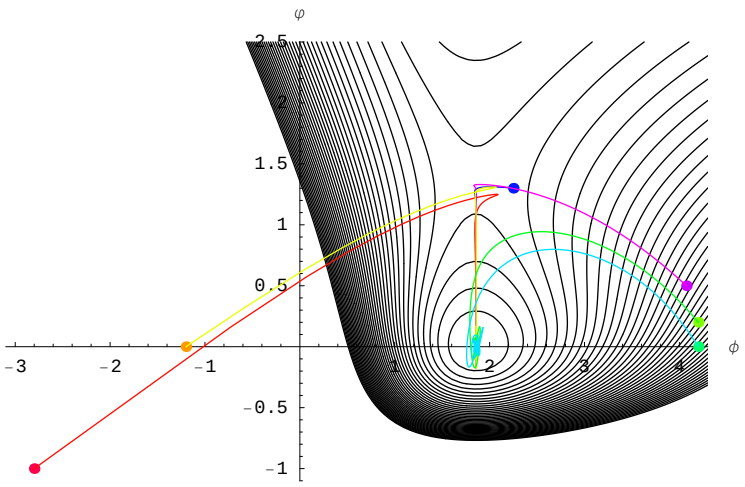

FIG. 2: Contour plot of the effective potential $U_{eff}(\varphi,\phi)$ (3.1) with potential $U(\phi)$ of the form (3.7) for parameters $d_1 = 1\,, \xi\Lambda_D = 1$ and relations $U(\phi_0) = f_1^2 = \lambda/2$. This plot clearly shows the global minimum and the saddle. The colored lines describe trajectories for scalar fields starting at different initial conditions.

the slow-roll parameters are[8]:

$$\epsilon \approx \eta_1 \approx \eta_2 \approx \frac{q}{2} + \frac{q_1}{2} \qquad (3.11)$$

and satisfy the slow-roll conditions $\epsilon, \eta_1, \eta_2 < 1$. As far as we know, there are no analytic solutions for such two-scalar-field potential. Anyway, from the form of the potential (3.10) and condition $q > q_1$ we can get an estimate $a \approx t^s$ with $s \gtrsim 2/q$ (e.g. $2/q = 3, 2, 5/3$ for $d_1 = 1, 2, 3$, respectively). Thus, in these regions we can get a period of power-law inflation. In spite of a rude character of these estimates, we shall see below that external space scale factors undergo power-law inflation for trajectories passing through these regions.

Now, we investigate dynamical behavior of scalar fields and the external space scale factor in more detail. There are no analytic solutions for considered model. So, we use numerical calculations. To do it, we apply a Mathematica package proposed in [36] adjusting it to our models and notations (see Appendix A).

The colored lines on the contour plot of the effective potential in Fig. 2 describe trajectories for scalar fields φ and ϕ with different initial values (the colored dots). The time evolution of these scalar fields[9] is drawn in Fig. 3. Here, the time t is measured in the Planck times and classical evolution starts at $t = 1$. For given initial conditions, scalar fields approach the global minimum of the effective potential along spiral trajectories.

We plot in Figure 4 the evolution of the logarithms of the scale factor $a(t)$ (left panel) and the evolution of the Hubble parameter $H(t)$ (right panel) and in Fig. 5 the evolution of the parameter of acceleration $q(t)$.

Because for initial condition we use the value $a(t = 1) = 1$ (in the Planck units), then $\log a(t)$ gives the number of e-folds: $\log a(t) = N(t)$. The Figure 4 shows that for considered trajectories we can reach the maximum of e-folds of the order of 10. Clearly, 10 e-folds is not sufficient to solve the horizon and flatness problems but it can be useful to explain a part of the modern CMB data. For example, the Universe inflates by $\triangle N \approx 4$ during the period that wavelengths corresponding to the CMB multipoles $2 \leq l \leq 100$ cross the Hubble radius [37]. However, to have the inflation which is long enough for all modes which contribute to the CMB to leave the horizon, it is usually supposed that $\triangle N \geq 15$ [38].

The Figure 4 for the evolution of the Hubble parameter (right panel) demonstrates that the red, yellow, dark blue and pink lines have a plateau $H \approx const$. It means that the scale factor $a(t)$ has a stage of the De Sitter expansion on these plateaus. Clearly, it happens because these lines reach the vicinity of the effective potential saddle point and spend there some time.

[8] In the case of n scalar fields $\varphi_i\,(i = 1, \ldots, n)$ with a flat ($\sigma-$model) target space, the slow-roll parameters for the spatially flat Friedmann Universe read (see e.g. [7, 13]): $\epsilon \equiv \frac{2}{H^2}\sum_{i=1}^n (\partial_i H)^2 \approx \frac{1}{2}|\partial U|^2/U^2$; $\eta_i \equiv -\ddot{\varphi}_i/(H\dot{\varphi}_i) = 2\partial_{ii}^2 H/H \approx -\epsilon + \sum_{j=1}^n \partial_{ij}^2 U \partial_j U/(U\partial_i U)$, where $\partial_i := \partial/\partial\varphi_i$ and $|\partial U|^2 = \sum_{i=1}^n (\partial_i U)^2$. In some papers (see e.g. [35]) it was introduced a "cumulative" parameter $\eta \equiv -\sum_{i=1}^n \ddot{\varphi}_i\dot{\varphi}_i/(H|\dot{\varphi}|^2) \approx -\epsilon + \sum_{i,j=1}^n (\partial_{ij}^2 U)(\partial_i U)(\partial_j U)/(U|\partial U|^2)$, where $|\dot{\varphi}|^2 = \sum_{i=1}^n \dot{\varphi}_i^2$. We can easily find that for the potential (3.10) parameter η coincides exactly with parameters η_1 and η_2.

[9] We remind that φ describes fluctuations of the internal space scale factor and ϕ reflects the additional degree of freedom of the original nonlinear theory.

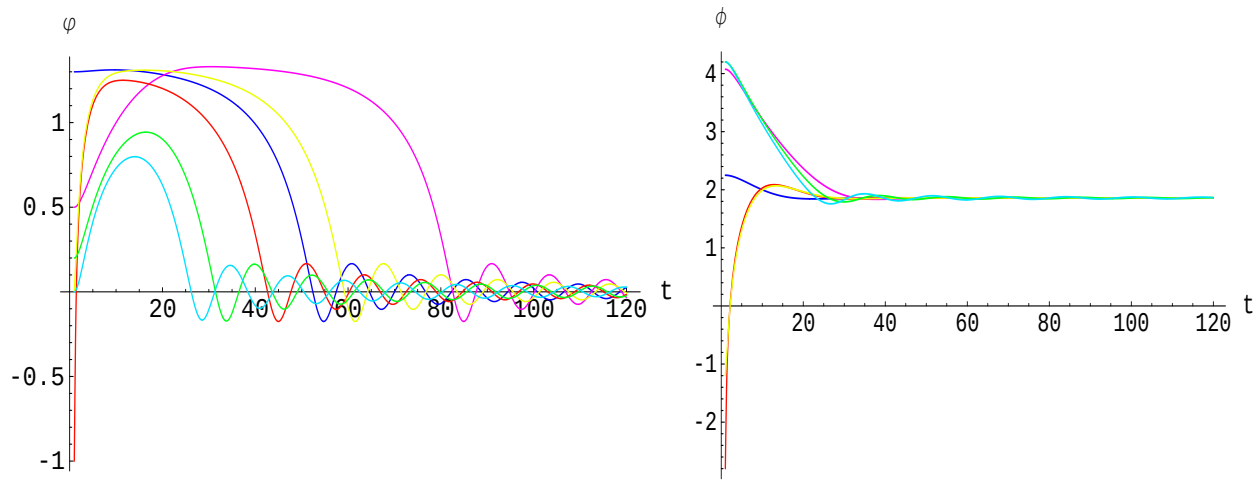

FIG. 3: Dynamical behavior of scalar fields φ (left panel) and ϕ (right panel) with corresponding initial values denoted by the colored dots in Fig. 2.

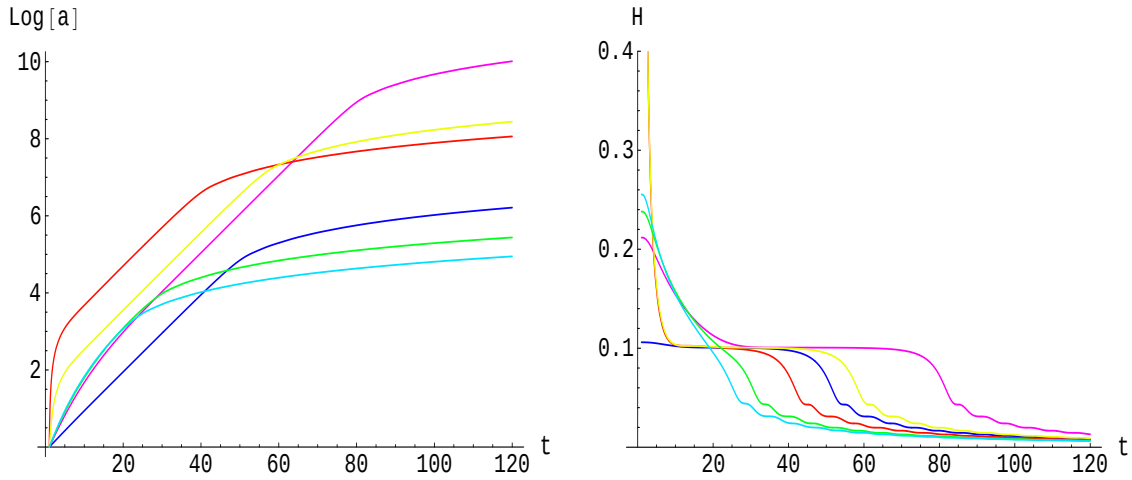

FIG. 4: The number of e-folds (left panel) and the Hubble parameter (right panel) for the corresponding trajectories.

The Fig. 5 for the acceleration parameter defined in (A.6) confirms also the above conclusions. According to Eq. (A.8), $q = 1$ for the De Sitter-like behavior. Indeed, all these 4 lines have stages $q \approx 1$ for the same time intervals when H has a plateau. Additionally, the magnification of this picture at early times (the right panel of the Figure 5) shows that pink, green and blue lines have also a period of time when q is approximately constant less than one: $q \approx 0.75$. In accordance with Eq. (A.8), it means that during this time the scale factor $a(t)$ undergoes the power-law inflation $a(t) \propto t^s$ with $s \approx 4$. This result confirms our rude estimates made above for the trajectories which go through the regions where the effective potential has the form (3.10). After stages of the inflation, the acceleration parameter starts to oscillate. Averaging q over a few periods of oscillations, we obtain $\bar{q} = -0.5$. Therefore, the scale factor behaves as for the matter dominated Universe: $a(t) \propto t^{2/3}$. Clearly, it corresponds to the times when the trajectories reach the vicinity of the effective potential global minimum and start to oscillate there. It is worth of noting, that there is no need to plot dynamical behavior for the equation of state parameter $\omega(t)$ because it is linearly connected with q (see Eq. (A.7)) and its behavior can be easily understood from the pictures for $q(t)$.

As we have seen above for considered quadratic model, the maximal number of e-folds is near 10. Can we increase this number? To answer this question, we shall consider a new model with a higher degree of nonlinearity, i.e. the nonlinear quartic model.

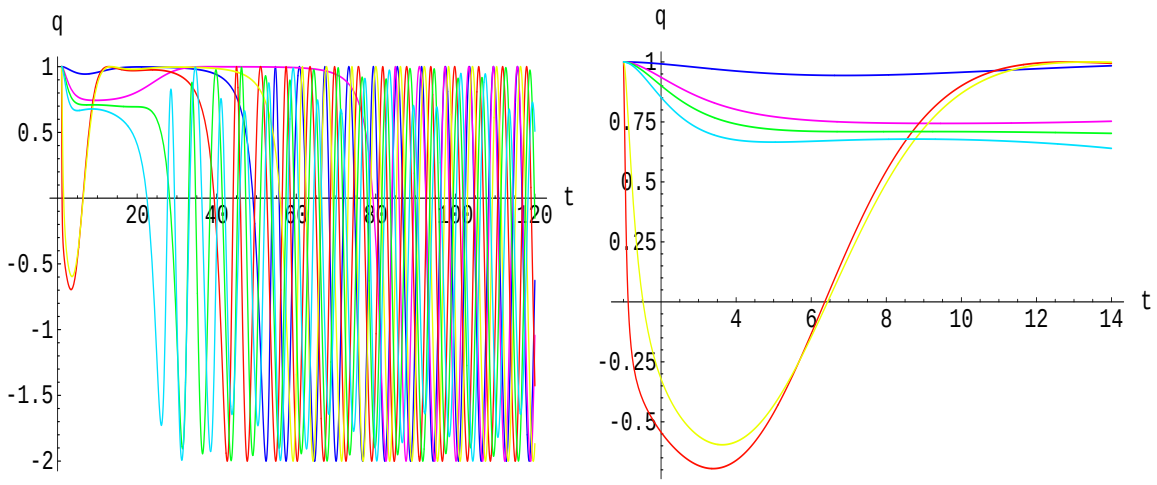

FIG. 5: The parameter of acceleration (left panel) and its magnification for early times (right panel). There are two different form of acceleration with $q \approx 1$ (De Sitter-like inflation) and $q \approx 0.75$ (power-law inflation with $s \approx 4$) accordingly. The averaging of q over a few periods of oscillations results in $\bar{q} = -0.5$ which corresponds to the matter dominated decelerating Universe.

IV. NONLINEAR QUARTIC MODEL

In this section we consider the nonlinear quartic model

$$f(\bar{R}) = \bar{R} + \gamma \bar{R}^4 - 2\Lambda_D \,. \tag{4.1}$$

For this model the scalar field potential (3.4) reads [11]:

$$U(\phi) = \frac{1}{2} e^{-B\phi} \left[\frac{3}{4} (4\gamma)^{-1/3} (e^{A\phi} - 1)^{4/3} + 2\Lambda_D \right] . \tag{4.2}$$

Here, the scalar curvature $\bar{R}$ and scalar field ϕ are connected as follows: $e^{A\phi} \equiv f' = 1 + 4\gamma \bar{R}^3 \quad \Leftrightarrow \quad \bar{R} = \left[(e^{A\phi} - 1)/4\gamma \right]^{1/3}$.

We are looking for a solution which has a nonnegative minimum of the effective potential $U_{eff}(\varphi, \phi)$ (3.1) where potential $U(\phi)$ is given by Eq. (4.2). If ϕ_0 corresponds to this minimum, then, as we mentioned above (see also [22]), $U(\phi_0), \lambda$ and f_1^2 should be positive. To get zero minimum of the effective potential, these positive values should satisfy the relation of the form of (2.8): $U(\phi_0) = f_1^2 = \lambda/2$. Additionally, it is important to note that positiveness of $U(\phi_0)$ results in positive expression for $\bar{R}(\phi_0) > 0$ [11].

Eq. (4.2) shows that potential $U(\phi)$ has the following asymptotes for positive γ and Λ_D[10] : $\phi \to -\infty \Longrightarrow U(\phi) \approx \frac{1}{2} e^{-B\phi} \left[\frac{3}{4} (4\gamma)^{-1/3} + 2\Lambda_D \right] \to +\infty$ and $\phi \to +\infty \Longrightarrow U(\phi) \approx \frac{3}{8} (4\gamma)^{-1/3} e^{(-B+4A/3)\phi} \to +0$. For the latter asymptote we took into account that $-B + 4A/3 = (D-8)/3\sqrt{(D-2)(D-1)} < 0$ for $D < 8$. Obviously, the total number of dimensions $D = 8$ plays the critical role in quartic nonlinear theories (see [11, 14, 39]) and investigations for $D < 8, D = 8$ and $D > 8$ should be performed separately. To make our paper is not too cumbersome, we consider the case $D < 8$ (i.e. $d_1 = 1, 2, 3$), postponing other cases for our following investigations.

It is worth of noting that for considered signs of parameters, the effective potential $U_{eff}(\varphi, \phi)$ (3.1) acquires negative values when $\phi \to +\infty$ (and $U(\phi) \to 0$). For example, if $U(\phi_0) = f_1^2 = \lambda/2$ (the case of zero minimum of the effective potential), the effective potential $U_{eff}(\varphi, \phi \to \infty) < 0$ for $0 < e^{-b\varphi} < 2$ and the lowest negative asymptotic value $U_{eff}|_{min} \to -(16/27)\lambda$ takes place along the line $e^{-b\varphi} = 4/3$. Therefore, zero minimum of U_{eff} is local[11].

As we mentioned above, extremum positions ϕ_i of the potential $U(\phi)$ coincide with extremum positions of $U_{eff}(\varphi, \phi)$: $dU/d\phi|_{\phi_i} = 0 \to \partial_\phi U_{eff}|_{\phi_i} = 0$. The condition of extremum for the potential $U(\phi)$ reads:

$$\frac{dU}{d\phi} = 0 \implies \bar{R}^4 - \frac{(2+d_1)}{\gamma(4-d_1)} \bar{R} + 2\Lambda_D \frac{(4+d_1)}{\gamma(4-d_1)} = 0 \,. \tag{4.3}$$

[10] Negative values of Λ_D and γ may lead either to negative minima, resulting in asymptotically AdS Universe, or to infinitely large negative values of U_{eff} [11]. In the present paper we want to avoid both of these possibilities. Therefore, we shall consider the case of $\Lambda_D, \gamma > 0$. See also footnote 12.

[11] It is not difficult to show that the thin shell approximation is valid for considered model and a tunnelling probability from the zero local minimum to this negative U_{eff} region is negligible.

For positive γ and Λ_D this equation has two real roots:

$$\bar{R}_{0(1)} = \frac{\Lambda_D}{2}\left(-\sqrt{\frac{2(2+d_1)}{(4-d_1)k\sqrt{M}} - M} + \sqrt{M}\right), \tag{4.4}$$

$$\bar{R}_{0(2)} = \frac{\Lambda_D}{2}\left(\sqrt{\frac{2(2+d_1)}{(4-d_1)k\sqrt{M}} - M} + \sqrt{M}\right), \tag{4.5}$$

where we introduced a dimensionless parameter

$$k := \gamma\Lambda_D^3\,, \tag{4.6}$$

which is positive for positive γ and Λ_D, and quantities $M,\ \omega$ read

$$M \equiv -2^{10/3}\frac{(4+d_1)}{\omega^{1/3}} - \frac{1}{3\cdot 2^{1/3}k}\frac{\omega^{1/3}}{(4-d_1)}\,, \tag{4.7}$$

$$\omega \equiv k\left[-27(4-d_1)(2+d_1)^2 + \sqrt{27^2(4-d_1)^2(2+d_1)^4 - 4\cdot 24^3 k(16-d_1^2)^3}\right]. \tag{4.8}$$

It can be easily seen that for $k>0$ we get $\omega<0$ and $M\geq 0$. To have real ω, parameter k should satisfy the following condition

$$k \leq \frac{27^2(4-d_1)^2(2+d_1)^4}{4\cdot 24^3(16-d_1^2)^3} \equiv k_0\,. \tag{4.9}$$

It is not difficult to verify that roots $\bar{R}_{0(1,2)}$ are real and positive if $0<k\leq k_0$ and they degenerate for $k\to k_0$: $\bar{R}_{0(1,2)} \to (\Lambda_D/2)\sqrt{M}$. In this limit the minimum and maximum of $U(\phi)$ merge into an inflection point. Now, we should define which of these roots corresponds to minimum of $U(\phi)$ and which to local maximum. The minimum condition

$$\left.\frac{d^2U(\phi)}{d\phi^2}\right|_{\phi_0} > 0 \implies \gamma\left[(d_1+2) - 4\gamma\bar{R}_0^3(4-d_1)\right] > 0 \tag{4.10}$$

results in the following inequality[12]:

$$\gamma>0\ :\quad (d_1+2) - 4\gamma\bar{R}_0^3(4-d_1) > 0\,. \tag{4.11}$$

Thus, the root $\bar{R}_0$ which corresponds to the minimum of $U(\phi)$ should satisfy the following condition:

$$0 < \bar{R}_0 < \left(\frac{d_1+2}{4\gamma(4-d_1)}\right)^{1/3}. \tag{4.12}$$

[12] As we have already mentioned above, the condition $U(\phi_0)>0$ leads to the inequality $\bar{R}(\phi_0)>0$ [11]. Taking into account the condition $d_1<4$, we clearly see that inequality $(d_1+2)+4|\gamma|\bar{R}_0^3(4-d_1)<0$ for $\gamma<0$ cannot be realized. This is an additional argument in favor of positive sign of γ.

Numerical analysis shows that $\bar{R}_{0(1)}$ satisfies these conditions and corresponds to the minimum. For $\bar{R}_{0(2)}$ we obtain that $\bar{R}_{0(2)} > \left(\frac{d_1+2}{4\gamma(4-d_1)}\right)^{1/3}$ and corresponds to the local maximum of $U(\phi)$. In what follows we shall use the notations:

$$\phi_{min} = \frac{1}{A}\ln\left[1+4\gamma\bar{R}_{0(1)}^3\right], \tag{4.13}$$

$$\phi_{max} = \frac{1}{A}\ln\left[1+4\gamma\bar{R}_{0(2)}^3\right] \tag{4.14}$$

and $U(\phi_{min})\equiv U_{min}\,, U(\phi_{max})\equiv U_{max}$. We should note that $\phi_{min}\,,\phi_{max}$ and the ratio U_{max}/U_{min} depend on the combination k (4.6) rather than on γ and Λ_D taken separately.

Obviously, because potential $U(\phi)$ has two extrema at ϕ_{min} and ϕ_{max}, the effective potential $U_{eff}(\varphi,\phi)$ may have points of extrema only on the lines $\phi=\phi_{min}$ and $\phi=\phi_{max}$ where $\partial U_{eff}/\partial\phi|_{\phi_{min},\phi_{max}}=0$. To find these extrema of U_{eff}, it is necessary to consider the second extremum condition $\partial U_{eff}/\partial\varphi = 0$ on each line separately:

$$\frac{\partial U_{eff}}{\partial\varphi} = 0 \Longrightarrow \begin{cases} -U_{min} - 3f_1^2\chi_1^2 + 2\lambda\chi_1 = 0\,, \\ -U_{max} - 3f_1^2\chi_2^2 + 2\lambda\chi_2 = 0\,, \end{cases} \tag{4.15}$$

where $\chi_1 \equiv \exp\left(-\sqrt{2d_1/(d_1+2)}\,\varphi_1\right) > 0$ and $\chi_2 \equiv \exp\left(-\sqrt{2d_1/(d_1+2)}\,\varphi_2\right) > 0$; φ_1 and φ_2 denote positions of extrema on the lines $\phi=\phi_{min}$ and $\phi=\phi_{max}$, respectively. These equations have solutions

$$\chi_{1(\pm)} = \alpha \pm \sqrt{\alpha^2-\beta}\,, \quad \alpha \geq \sqrt{\beta} \equiv \alpha_1\,; \tag{4.16}$$

$$\chi_{2(\pm)} = \alpha \pm \sqrt{\alpha^2 - \beta\frac{U_{max}}{U_{min}}}\,, \quad \alpha \geq \sqrt{\beta\frac{U_{max}}{U_{min}}} \equiv \alpha_2 > \alpha_1\,; \tag{4.17}$$

where we have introduced the notations: $\alpha\equiv\lambda/(3f_1^2)$ and $\beta\equiv U_{min}/(3f_1^2)$. These equations show that there are 5 different possibilities which are listed in the Table I.

To clarify which of solutions (4.16) and (4.17) correspond to minima of the effective potential (with respect to φ) we should consider the minimum condition

$$\left.\frac{\partial^2 U_{eff}}{\partial^2\varphi}\right|_{min} > 0 \quad\Longrightarrow\quad U_{extr} + \chi^2 9f_1^2 - 4\lambda\chi > 0\,, \tag{4.18}$$

where U_{extr} is either U_{min} or U_{max} and χ denotes either χ_1 or χ_2. Taking into account relations (4.15), we obtain

$$\chi^2 3f_1^2 - \chi\lambda > 0 \quad\Longrightarrow\quad \chi > \frac{\lambda}{3f_1^2} = \alpha. \tag{4.19}$$

TABLE I: The number of extrema of the effective potential U_{eff} depending on the relation between parameters.

$0<\alpha<\alpha_1$	$\alpha=\alpha_1$	$\alpha_1<\alpha<\alpha_2$	$\alpha=\alpha_2$	$\alpha>\alpha_2$
no extrema	**one extremum** (point of inflection on the line $\phi=\phi_{min}$)	**two extrema** (one minimum and one saddle on the line $\phi=\phi_{min}$)	**three extrema** (minimum and saddle on the line $\phi=\phi_{min}$, inflection on the line $\phi=\phi_{max}$)	**four extrema** (minimum and saddle on the line $\phi=\phi_{min}$ maximum and saddle on the line $\phi=\phi_{max}$)

Thus, roots $\chi_{1,2(+)}$ define the positions of local minima of the effective potential with respect to the variable φ and $\chi_{1,2(-)}$ correspond to local maxima (in the direction of φ).

Now, we fix the minimum $\chi_{1(+)}$ at the point $\varphi=0$. It means that in this local minimum the internal space scale factor is stabilized at the present day value. In this case

$$\chi_{1(+)}\big|_{\varphi=0}=1=\alpha+\sqrt{\alpha^2-\beta}\quad\Longrightarrow\quad\alpha=\frac{1+\beta}{2}\,. \tag{4.20}$$

Obviously, we can do it only if[13] $\alpha<1\Rightarrow\beta\in[0,1)$. For $\chi_{1(-)}$ we get: $\chi_{1(-)}=\beta$.

Additionally, the local minimum of the effective potential at the point $(\varphi=0,\phi=\phi_{min})$ should play the role of the nonnegative four-dimensional effective cosmological constant. Thus, we arrive at the following condition:

$$\begin{aligned}\Lambda_{eff}&\equiv U_{eff}(\varphi=0,\phi=\phi_{min})\\&=-\lambda+U_{min}+f_1^2\geq 0\\&\Longrightarrow\ -\alpha+\beta+\frac{1}{3}\geq 0\,.\end{aligned}\tag{4.21}$$

From the latter inequality and equation (4.20) we get $\beta\in\left[\frac{1}{3},1\right)$. It can be easily seen that $\beta=1/3$ (and, correspondingly, $\alpha=2/3$) results in $\Lambda_{eff}=0$ and we obtain the mentioned above relations: $U_{min}=f_1^2=\lambda/2$. In general, it is possible to demand that Λ_{eff} coincides with the present day dark energy value $10^{-57}\mathrm{cm}^{-2}$. However, it leads to very flat local minimum which means the decompactification of the internal space [22]. In what follows, we shall mainly consider the case of zero Λ_{eff} although all obtained results are trivially generalized to $\Lambda_{eff}=10^{-57}\mathrm{cm}^{-2}$.

Summarizing our results, in the most interesting case of $\alpha>\alpha_2$ the effective potential has four extrema: local minimum at $\left(\varphi|_{\chi_{1(+)}}=0,\phi_{min}\right)$, local maximum at $\left(\varphi|_{\chi_{2(-)}},\phi_{max}\right)$ and two saddle-points at $\left(\varphi|_{\chi_{1(-)}},\phi_{min}\right)$, and $\left(\varphi|_{\chi_{2(+)}},\phi_{max}\right)$ (see Fig. 7).

We pay particular attention to the case of zero local minimum $U_{eff}(\varphi|_{\chi_{1(+)}}=0,\phi_{min})=0$ where $\beta=1/3\Longrightarrow\alpha=(1+\beta)/2=2/3$. To satisfy the four-extremum condition $\alpha>\alpha_2$, we should demand

$$\frac{U_{max}}{U_{min}}<\frac{4}{3}\,. \tag{4.22}$$

The fraction U_{max}/U_{min} is the function of k and depends parametrically only on the internal space dimension d_1. Inequality (4.22) provides the lower bound on k and numerical analysis (see Fig. 6) gives

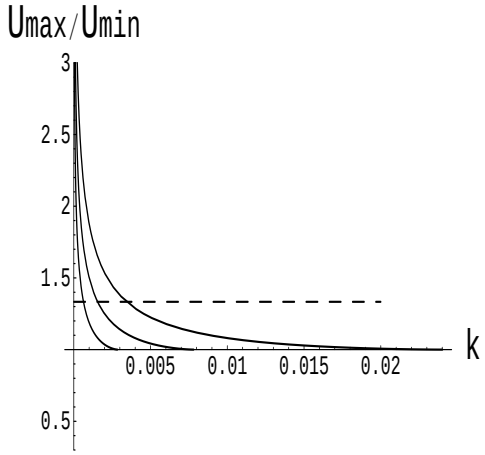

FIG. 6: The form of U_{max}/U_{min} as a function of $k\in(0,k_0]$ for $d_1=1,2,3$ from left to right, respectively. Dashed line corresponds to $U_{max}/U_{min}=4/3$.

$\tilde{k}(d_1=1)\approx 0.000625$; $\tilde{k}(d_1=2)\approx 0.00207$; $\tilde{k}(d_1=3)\approx 0.0035$. Therefore, effective potentials with zero local minimum will have four extrema if $k\in(\tilde{k},k_0)$ (where k_0 is defined by Eq. (4.9)). The limit $k\to\tilde{k}$ results in merging $\chi_{2(-)}\leftrightarrow\chi_{2(+)}$ and the limit $k\to k_0$ results in merging $\chi_{1(-)}\leftrightarrow\chi_{2(-)}$ and $\chi_{1(+)}\leftrightarrow\chi_{2(+)}$. Such merging results in transformation of corresponding extrema into inflection points. For example, from Fig. 6 follows that $U_{max}/U_{min}\to 1$ for $k\to k_0$.

[13] Particular value $\alpha=1$ corresponds to the case $\alpha=\alpha_1=1$ where the only extremum is the inflection point with $\chi_{1(-)}=\chi_{1(+)}=\alpha=1$. Here, $\lambda=U_{min}=3f_1^2$ and $U_{eff}(\varphi=0,\phi=\phi_{min})=-\lambda+U_{min}+f_1^2>0$.

The typical contour plot of the effective potential with four extrema in the case of zero local minimum is drawn in Fig. 7. Here, for $d_1 = 3$ we take $k = 0.004 \in (\tilde{k}, k_0)$ which gives $\alpha_2 \approx 0.655$. Thus, $\alpha = 2/3 \approx 0.666 > \alpha_2$.

Let us investigate now a possibility of inflation for considered potential. First of all, taking into account the comments in previous section (see a paragraph before Eq. (3.9)), it is clear that topological inflation in the saddle point $\chi_{1(-)}$ as well as the slow rolling from there in the direction of the local minimum $\chi_{1(+)}$ are absent. It is not difficult to verified that the generalized power-low inflation discussed in the case of the nonlinear quadratic model is also absent here. Indeed, from Eqs. (3.1) and (4.2) follows that nonlinear potential $U(\phi)$ can play the leading role in the region $\phi \to -\infty$ (because $U(\phi) \to 0$ for $\phi \to +\infty$). In this region $U_{eff} \propto \exp(-\sqrt{q}\varphi)\exp(-\sqrt{q_2}\phi)$ where $q = 2d_1/(d_1+2)$ and $q_2 = B^2 = (d_1+4)^2/[(d_1+2)(d_1+3)]$. For these values of q and q_2 the slow-roll conditions are not satisfied: $\epsilon \approx \eta_1 \approx \eta_2 \approx q/2 + q_2/2 > 1$. However, there are two promising regions where the stage of inflation with subsequent stable compactification of the internal space may take place. We mean the local maximum $\chi_{2(-)}$ and the saddle $\chi_{2(+)}$ (see Fig. 7). Let us estimate the slow roll parameters for these regions.

We consider first the local maximum $\chi_{2(-)}$. It is obvious that the parameter ϵ is equal to zero here. Additionally, from the form of the effective potential (3.1) it is clear that the mixed second derivatives are also absent in extremum points. Thus, the slow roll parameters η_1 and η_2, defined in the footnote (8), coincide exactly with η_φ and η_ϕ. In Fig. 8 we present typical form of these parameters as functions of $k \in (\tilde{k}, k_0)$ in the case $\beta = 1/3$ and $d_1 = 1, 2, 3$. These plots show that, for considered parameters, the slow roll inflation in this region is possible for $d_1 = 1, 3$.

The vicinity of the saddle point $\chi_{2(+)}$ is another promising region. Obviously, if we start from this point, a test particle will roll mainly along direction of ϕ. That is why it makes sense to draw only $|\eta_\phi|$. In Fig. 9 we plot typical form of $|\eta_\phi|$ in the case $\beta = 1/3$ and $d_1 = 1, 2, 3$. Left panel represents general behavior for the whole range of $k \in (\tilde{k}, k_0)$ and right panel shows detailed behavior in the most interesting region of small k. It shows that $d_1 = 3$ is the most promising case in this region.

Now, we investigate numerically the dynamical behavior of scalar fields and the external space scale factor for trajectories which start from the regions $\chi_{1(-)}, \chi_{2(-)}$ and $\chi_{2(+)}$. All numerical calculations perform for $\beta = 1/3, d_1 = 3$ and $k = 0.004$. The colored lines on the contour plot of the effective potential in Fig. 7 describe trajectories for scalar fields φ and ϕ with different initial values (the colored dots) in the vicinity of these extrema points. The time evolution of these scalar fields is drawn in Fig. 10. For given initial conditions, scalar fields approach the local minimum $\chi_{1(+)}$ of the effective potential along the spiral trajectories.

We plot in Figure 11 the evolution of the logarithm of the scale factor $a(t)$ (left panel) which gives directly the number of e-folds and the evolution of the Hubble parameter $H(t)$ (right panel) and in Fig. 12 the evolution of the parameter of acceleration $q(t)$.

The Figure 11 shows that for considered trajectories we can reach the maximum of e-folds of the order of 22 which is long enough for all modes which contribute to the CMB to leave the horizon.

The Figure 11 for the evolution of the Hubble parameter (right panel) demonstrates that all lines have plateaus $H \approx const$. However, the red, yellow and blue lines which pass in the vicinity of the saddle $\chi_{2(+)}$ have bigger value of the Hubble parameter with respect to the dark blue line which starts from the $\chi_{1(-)}$ region. Therefore, the scale factor $a(t)$ has stages of the De Sitter-like expansion corresponding to these plateaus which last approximately from 100 (dark blue line) up to 800 (red line) Planck times.

The Fig. 12 for the acceleration parameter confirms also the above conclusions. All 4 lines have stages $q \approx 1$ for the same time intervals when H has plateaus. After stages of inflation, the acceleration parameter starts to oscillate. Averaging q over a few periods of oscillations, we obtain $\bar{q} = -0.5$. Therefore, the scale factor behaves as for the matter dominated Universe: $a(t) \propto t^{2/3}$. Clearly, it corresponds to the times when the trajectories reach the vicinity of the effective potential local minimum $\chi_{1(+)}$ and start to oscillate there.

Let us investigate now a possibility of the topological inflation [16, 40] if scalar fields φ, ϕ stay in the vicinity of the saddle point $\chi_{2(+)}$. As we mentioned in Section 2, topological inflation in the case of the double-well potential takes place if the distance between a minimum and local maximum bigger than $\Delta\phi_{cr} = 1.65$. In this case domain wall is thick enough in comparison with the Hubble radius. The critical ratio of the characteristic thickness of the wall to the horizon scale in local maximum is $r_w H \approx |U/3\partial U_{\phi\phi}|^{1/2} \approx 0.48$ [27] and for topological inflation it is necessary to exceed this critical value. Therefore, we should cheque the saddle $\chi_{2(+)}$ from the point of these criteria.

In Fig. 13 (left panel) we draw the difference $\Delta\phi = \phi_{max} - \phi_{min}$ for the profile $\varphi = \varphi|_{\chi_{2(+)}}$ as a functions of $k \in (\tilde{k}, k_0)$ in the case $\beta = 1/3$ for dimensions $d_1 = 1, 2, 3$. This picture shows that this difference can exceed the critical value if the number of the internal dimensions is $d_1 = 2$ and $d_1 = 3$. Right panel of Fig. 13 confirms this conclusion. Here we consider the case $\beta = 1/3, \quad k = 0.004$ and $d_1 = 3$. For chosen values of the parameters, $\Delta\phi = 2.63$ which is considerably bigger than the critical value 1.65 and the ratio of the thickness of the wall to the horizon scale is 1.30 which again bigger than the critical value 0.48. Therefore, topological inflation can happen for considered model. Moreover, due to quantum fluctuations of scalar fields, inflating domain wall will have fractal structure: it will contain many other inflating domain walls and each of these domain walls again will contain new inflating domain walls and so on [16].

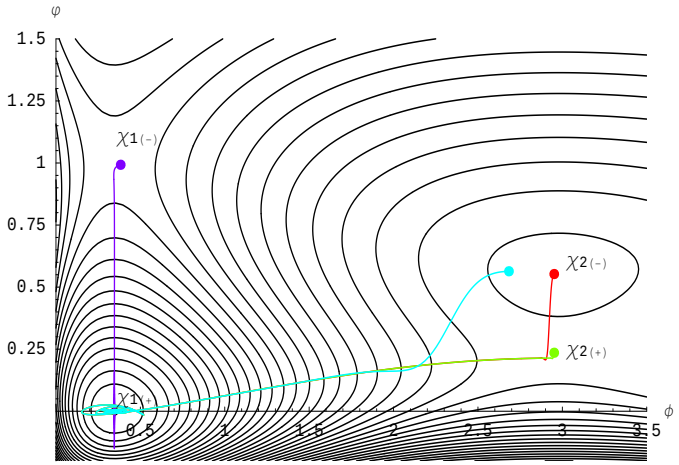

FIG. 7: Contour plot of the effective potential $U_{eff}(\varphi, \phi)$ (3.1) with potential $U(\phi)$ of the form (4.2) for parameters $\beta = 1/3$, $d_1 = 3$ and $k = 0.004$. This plot shows the local zero minimum, local maximum and two saddles. The colored lines describe trajectories for scalar fields starting at different initial conditions.

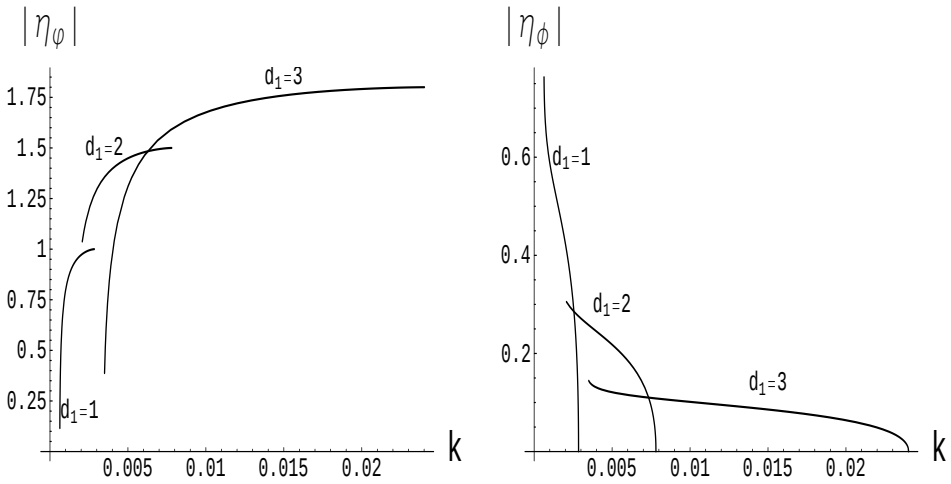

FIG. 8: Graphs of $|\eta_\varphi|$ (left panel) and $|\eta_\phi|$ (right panel) as functions of $k \in (\tilde{k}, k_0)$ for local maximum $\chi_{2(-)}$ and parameters $\beta = 1/3$ and $d_1 = 1, 2, 3$.

Thus, from this point, such topological inflation is the eternal one.

To conclude this section, we want to draw the attention to one interesting feature of the given model. From above consideration follows that in the case of zero minimum of the effective potential the positions of extrema are fully determined by the parameters k and d_1, and for fixed k and d_1 do not depend on the choice of Λ_D. The same takes place for the slow roll parameters. On the other hand, if we keep k and d_1, the hight of the effective potential is defined by Λ_D (see Appendix B). Therefore, we can change the hight of extrema with the help of Λ_D but preserve the conditions of inflation for given k and d_1.

However, the dynamical characteristics of the model (drawn in figures 10 - 12) depend on variations of Λ_D by the self-similar manner. It means that the change of hight of the effective potential via transformation $\Lambda_D \to c\Lambda_D$ (c is a constant) with fixed k and d_1 results in rescaling of figures 10 - 12 in $1/\sqrt{c}$ times along the time axis.

V. SUMMARY AND DISCUSSION

In our paper we investigated a possibility of inflation in multidimensional cosmological models. The main attention was paid to nonlinear (in scalar curvature) models with quadratic R^2 and quartic R^4 lagrangians. These models contain two scalar fields. One of them corresponds to the scale factor of the internal space and another one is related with the nonlinearity of the original models. The effective four-

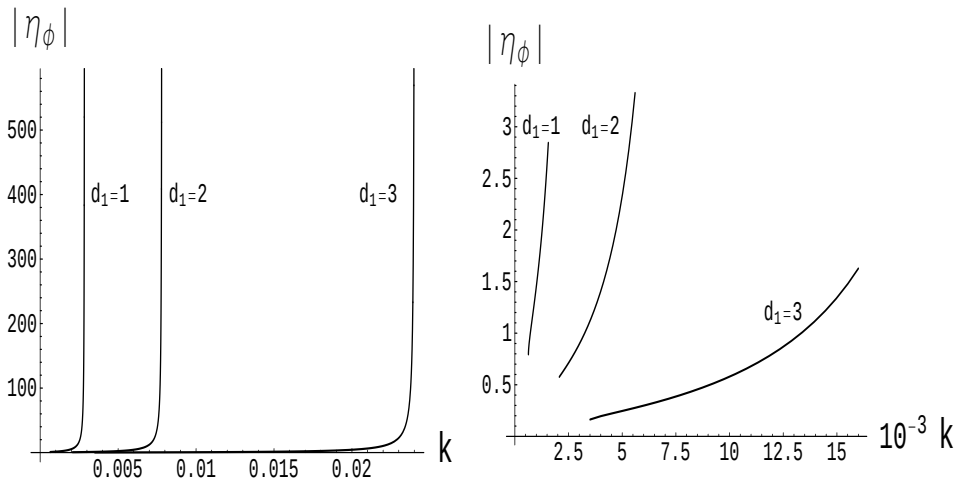

FIG. 9: Grafs of $|\eta_\phi|$ as functions of k for saddle point $\chi_{2(+)}$ and parameters $\beta = 1/3$ and $d_1 = 1, 2, 3$. Left panel demonstrates the whole region of variable $k \in (\tilde{k}, k_0)$ and right panel shows detailed behavior for small k.

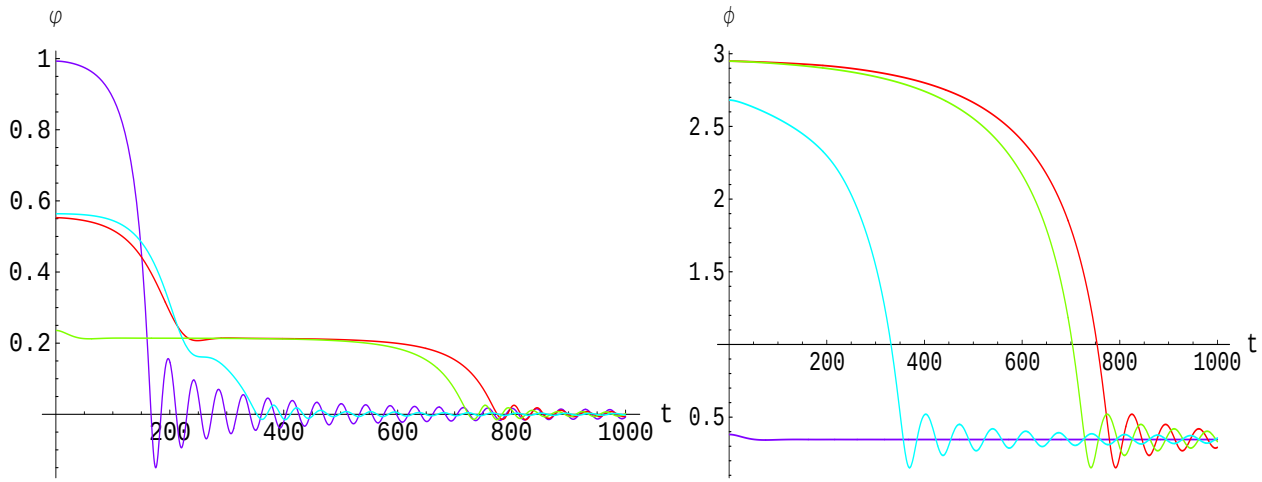

FIG. 10: Dynamical behavior of scalar fields φ (left panel) and ϕ (right panel) with corresponding initial values denoted by the colored dots in Fig. 7.

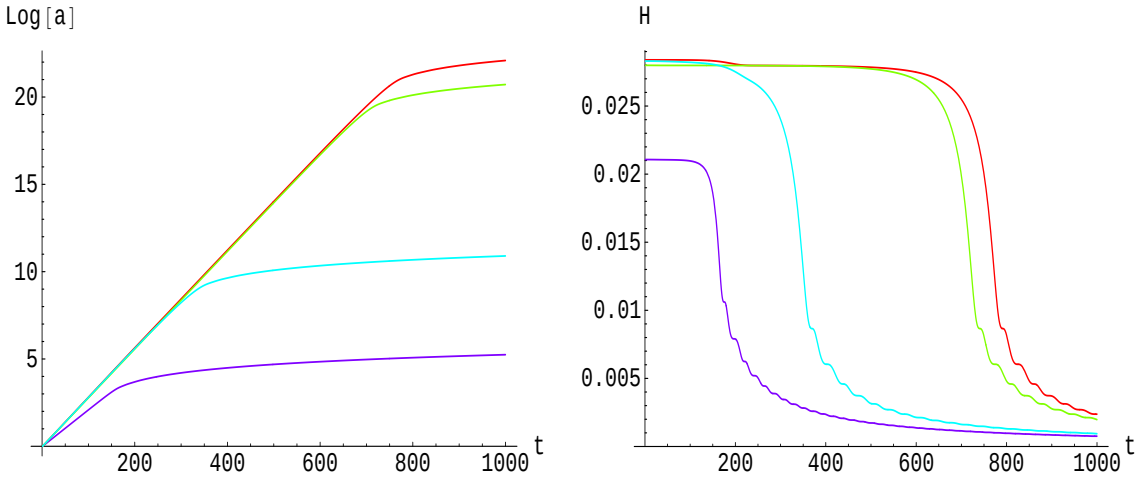

FIG. 11: The number of e-folds (left panel) and the Hubble parameter (right panel) for the corresponding trajectories.

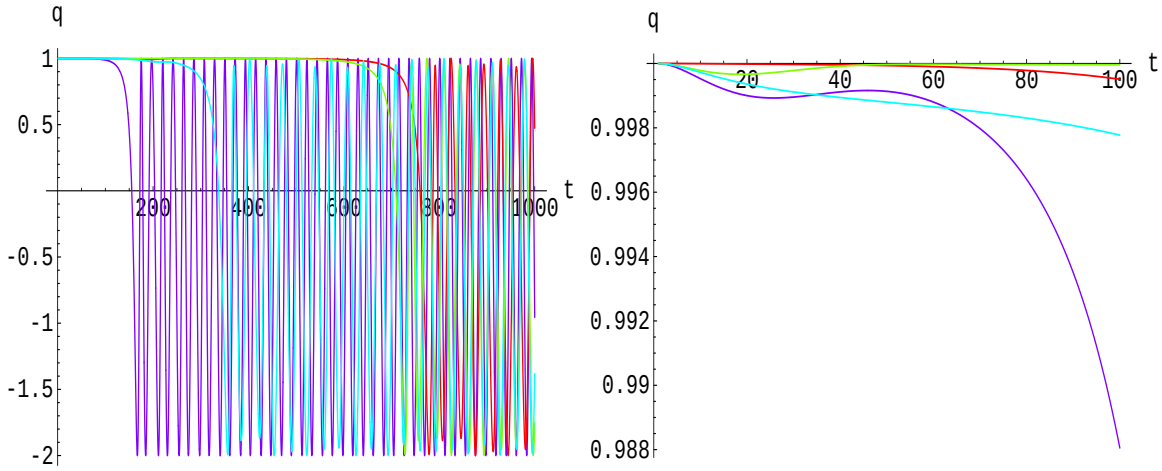

FIG. 12: The parameter of acceleration (left panel) and its magnification for early times (right panel).

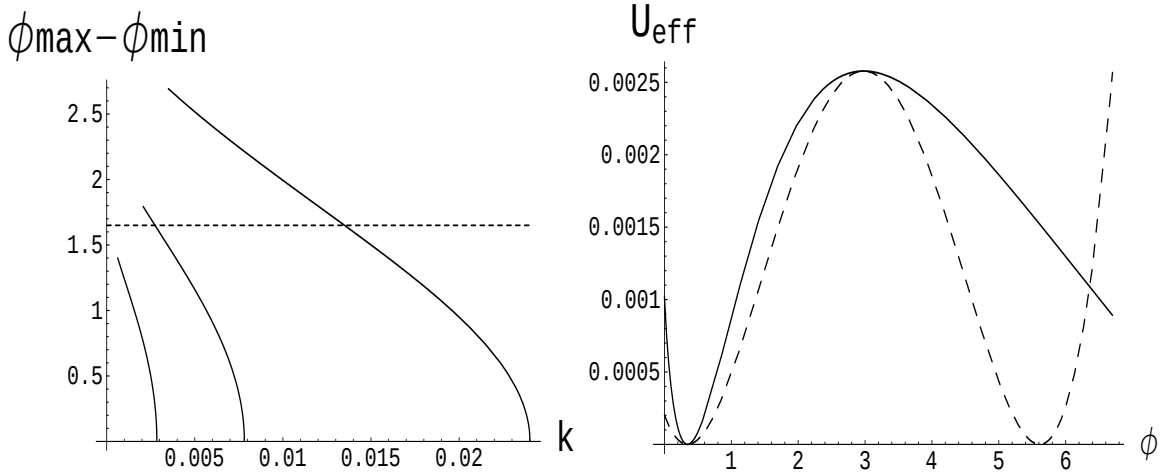

FIG. 13: Left panel demonstrates the difference $\phi_{max} - \phi_{min}$ (for the profile $\varphi = \varphi|_{\chi_{2(+)}}$) as a functions of $k \in (\tilde{k}, k_0)$ for parameters $\beta = 1/3$, and $d_1 = 1, 2, 3$ (from left to right respectively). Dashed line corresponds to $\phi_{max} - \phi_{min} = 1.65$. Right panel shows the comparison of the potential $U_{eff}(\varphi|_{\chi_{2(+)}}, \phi)$ with a double-well potential for parameters $\beta = 1/3, k = 0.004$ and $d_1 = 3$.

dimensional potentials in these models are fully determined by the geometry and matter content of the models. The geometry is defined by the direct product of the Ricci-flat external and internal spaces. As a matter source, we include a monopole form field, D-dimensional bare cosmological constant and tensions of branes located in fixed points. The exact form of the effective potentials depends on the relation between parameters of the models and can take rather complicated view with a number of extrema points.

First of all, we found a range of parameters which insures the existence of zero minima of the effective potentials. These minima provide sufficient condition to stabilize the internal space and, consequently, to avoid the problem of the fundamental constant variation. Zero minima correspond to the zero effective four-dimensional cosmological constant. In general, we can also consider positive effective cosmological constant which corresponds to the observable now dark energy. However, it usually requires extreme fine tuning of parameters of models.

Then, for corresponding effective potentials, we investigated the possibility of the external space inflation. We have shown that for some initial conditions in the quadratic and quartic models we can achieve up to 10 and 22 e-folds, respectively. An additionally bonus of the considered model is that R^4 model can provide conditions for the eternal topological inflation.

Obviously, 10 and 22 e-folds are not sufficient to solve the homogeneity and isotropy problem but big enough to explain the recent CMB data. To have the inflation which is long enough for modes which contribute to the CMB, it is usually supposed that $\triangle N \geq 15$ [38]. Moreover, 22 e-folds is rather big

number to encourage the following investigations of the nonlinear multidimensional models to find theories where this number will approach 50-60. We have seen that the increase of the nonlinearity (from quadratic to quartic one) results in the increase of $\triangle N$ in more that two times. So, there is a hope that more complicated nonlinear models can provide necessary 50-60 e-folds. Besides, this number is reduced in models where long matter dominated (MD) stage followed inflation can subsequently decay into radiation [42, 43]. Precisely this scenario takes place for our models. We have shown for quadratic and quartic nonlinear models, that MD stage with the external scale factor $a \sim t^{2/3}$ takes place after the stage of inflation. It happens when scalar fields start to oscillate near the position of zero minimum of the effective potential. However, scalar fields are not stable. For example, scalar field φ decays into two photons $\varphi \to 2\gamma$ with the decay rate $\Gamma \sim m_\varphi^3/M_{Pl}^2$ [30]. Thus the life time is $\tau_{decay} \sim (M_{Pl}/m_\varphi)^3 t_{Pl}$. The reheating temperature is given by the expression $T_{RH} \sim (m_\varphi^3/M_{Pl})^{1/2}$. Therefore, to get $T_{RH} \gtrsim 1$MeV necessary for the nucleosynthesis, we should take $m_\varphi \gtrsim 10$TeV. In paper [43], it is shown that for such scenario with intermediate MD stage, the necessary number of e-folds is reduced according to the formula:

$$\begin{aligned} \triangle N &= -\frac{1}{6}\ln\left(\frac{45}{2}g_*^{-3/2}\frac{m_\varphi^2}{\Gamma M_{Pl}}\right) \\ &= -\frac{1}{6}\ln\left(\frac{45}{2}g_*^{-3/2}\frac{M_{Pl}}{m_\varphi}\right), \end{aligned} \tag{5.1}$$

where g_* counts the effective number of relativistic degrees of freedom and we took into account that decaying particles are scalars. This expression weakly depends on g_*. For example, if $m_\varphi \sim 10$TeV we obtain $-6.27 \leq \triangle N \leq -5.11$ for $1 \leq g_* \leq 10^2$. Thus, $\triangle N \approx -6$. Therefore, we believe that the number of e-folds is not a big problem for multidimensional nonlinear models. The main problem consists in the spectral index. For example, in the case of R^4 model we get $n_s \approx 1 + 2\eta|_{\chi_{2(+)}} \approx 0.61$ which is less than observable now $n_s \approx 1$. A possible solution of this problem may consist in more general form of the nonlinearity $f(R)$. It was observed in [15] that simultaneous consideration quadratic and quartic nonlinearities can flatten the effective potential and increase n_s. We postpone this problem for our following investigations.

Acknowledgements

A. Zh. acknowledges the hospitality of the Theory Division of CERN where this work has been started. A.Zh. would like to thank the Abdus Salam International Center for Theoretical Physics (ICTP) for their kind hospitality during the final stage of this work.This work was supported in part by the "Cosmomicrophysics" programme of the Physics and Astronomy Division of the National Academy of Sciences of Ukraine.

APPENDIX A: FRIEDMANN EQUATIONS FOR MULTI-COMPONENT SCALAR FIELD MODEL

We consider n scalar fields minimally coupled to gravity in four dimensions. The effective action of this model reads

$$\begin{aligned} S &= \frac{1}{16\pi G}\int d^4x\sqrt{|\tilde{g}^{(0)}|}\Big(R[\tilde{g}^{(0)}] \\ &- G_{ij}\tilde{g}^{(0)\mu\nu}\partial_\mu\varphi^i\partial_\nu\varphi^j - 2U(\varphi^1,\varphi^2,\ldots)\Big) \end{aligned} \tag{A.1}$$

where the kinetic term is usually taken in the canonical form: $G_{ij} = \mathrm{diag}(1,1,\ldots)$ (flat σ model). Such multi-component scalar fields originate naturally in multidimensional cosmological models (with linear or nonlinear gravitational actions) [3, 7, 13]. We use the usual conventions $c = \hbar = 1$, i.e. $L_{Pl} = t_{Pl} = 1/M_{Pl}$ and $8\pi G = 8\pi/M_{Pl}^2$. Here, scalar fields are dimensionless and potential U has dimension $[U] = \mathrm{lehgth}^{-2}$.

Because we want to investigate dynamical behavior of our Universe in the presence of scalar fields, we suppose that scalar fields are homogeneous: $\varphi^i = \varphi^i(t)$ and four-dimensional metric is spatially-flat Friedmann-Robertson-Walker one: $\tilde{g}^{(0)} = -dt\otimes dt + a^2(t)d\vec{x}\otimes d\vec{x}$.

For energy density and pressure we easily get:

$$\begin{aligned} \rho &= \frac{1}{8\pi G}\left(\frac{1}{2}G_{ij}\dot{\varphi}^i\dot{\varphi}^j + U\right), \\ P &= \frac{1}{8\pi G}\left(\frac{1}{2}G_{ij}\dot{\varphi}^i\dot{\varphi}^j - U\right); \end{aligned} \tag{A.2}$$

$$\Longrightarrow \begin{cases} \frac{1}{2}G_{ij}\dot{\varphi}^i\dot{\varphi}^j = 4\pi G(\rho+P), \\ U = 4\pi G(\rho - P). \end{cases} \tag{A.3}$$

The Friedmann equations for considered model are

$$3\left(\frac{\dot{a}}{a}\right)^2 \equiv 3H^2 = 8\pi G\rho = \frac{1}{2}G_{ij}\dot{\varphi}^i\dot{\varphi}^j + U, \tag{A.4}$$

and

$$\dot{H} = -4\pi G(\rho+P) = -\frac{1}{2}G_{ij}\dot{\varphi}^i\dot{\varphi}^j. \tag{A.5}$$

From these 2 equations, we obtain the following expression for the acceleration parameter:

$$\begin{aligned} q &\equiv \frac{\ddot{a}}{H^2 a} = 1 - \frac{4\pi G}{H^2}(\rho+P) = -\frac{8\pi G}{6H^2}(\rho+3P) \\ &= \frac{1}{6H^2}\left(-4\times\frac{1}{2}G_{ij}\dot{\varphi}^i\dot{\varphi}^j + 2U\right). \end{aligned} \tag{A.6}$$

It can be easily seen that the equation of state (EoS) parameter $\omega = P/\rho$ and parameter q are linearly connected:

$$q = -\frac{1}{2}(1+3\omega)\,. \tag{A.7}$$

From the definition of the acceleration parameter, it follows that q is constant in the case of the power-law and De Sitter-like behavior:

$$q = \begin{cases} (s-1)/s\,; & a \propto t^s\,, \\ 1\,; & a \propto e^{Ht}\,. \end{cases} \tag{A.8}$$

For example, $q = -0.5$ during the matter dominated (MD) stage where $s = 2/3$.

Because the minisuperspace metric G_{ij} is flat, the scalar field equations are:

$$\ddot{\varphi}^i + 3H\dot{\varphi}^i + G^{ij}\frac{\partial U}{\partial \varphi^j} = 0\,. \tag{A.9}$$

For the action (A.1), the corresponding Hamiltonian is

$$\mathcal{H} = \frac{8\pi G}{2a^3}G^{ij}P_iP_j + \frac{a^3}{8\pi G}U\,, \tag{A.10}$$

where

$$P_i = \frac{a^3}{8\pi G}G_{ij}\dot{\varphi}^j \tag{A.11}$$

are the canonical momenta and equations of motion have also the canonical form

$$\dot{\varphi}^i = \frac{\partial \mathcal{H}}{\partial P_i}\,, \quad \dot{P}_i = -\frac{\partial \mathcal{H}}{\partial \varphi^i}\,. \tag{A.12}$$

It can be easily seen that the latter equation (for $\dot{P}_i$) is equivalent to the eq. (A.9).

Thus, the Friedmann equations together with the scalar field equations can be replaced by the system of the first order ODEs:

$$\dot{\varphi}^i = \frac{8\pi G}{a^3}G^{ij}P_j\,, \tag{A.13}$$

$$\dot{P}_i = -\frac{a^3}{8\pi G}\frac{\partial U}{\partial \varphi^i}\,, \tag{A.14}$$

$$\dot{a} = aH\,, \tag{A.15}$$

$$\dot{H} = \frac{\ddot{a}}{a} - H^2 = \frac{1}{6}\left(-4\times\frac{1}{2}G_{ij}\dot{\varphi}^i\dot{\varphi}^j + 2U\right) - H^2 \tag{A.16}$$

with Eq. (A.4) considered in the form of the initial conditions:

$$H(t=0) = \left.\sqrt{\frac{1}{3}\left(\frac{1}{2}G_{ij}\dot{\varphi}^i\dot{\varphi}^j + U\right)}\right|_{t=0}\,. \tag{A.17}$$

We can make these equations dimensionless:

$$\frac{d\varphi^i}{M_{Pl}dt} = \frac{8\pi}{M_{Pl}^3a^3}G^{ij}P_j,$$

$$\Rightarrow \frac{d\varphi^i}{dt} = \frac{8\pi}{a^3}G^{ij}P_j\,; \tag{A.18}$$

$$\frac{dP_i}{M_{Pl}dt} = -\frac{a^3M_{Pl}^3}{8\pi}\frac{\partial(U/M_{Pl}^2)}{\partial\varphi^i}\,,$$

$$\Rightarrow \frac{dP_i}{dt} = -\frac{a^3}{8\pi}\frac{\partial U}{\partial\varphi^i}\,. \tag{A.19}$$

That is to say the time t is measured in the Planck times t_{Pl}, the scale factor a is measured in the Planck lengths L_{Pl} and the potential U is measured in the M_{Pl}^2 units.

We use this system of dimensionless first order ODEs together with the initial condition (A.17) for numerical calculation of the dynamics of considered models with the help of a Mathematica package [36].

APPENDIX B: SELF-SIMILARITY CONDITION

Due to the zero minimum conditions $U(\phi_{min}) = f_1^2 = \lambda/2$, the effective potential (3.1) can be written in the form:

$$U_{eff}(\varphi,\phi) = U(\phi_{min})e^{-\sqrt{\frac{2d_1}{d_1+2}}\,\varphi} \times\left[\frac{U(\phi)}{U(\phi_{min})} + e^{-2\sqrt{\frac{2d_1}{d_1+2}}\,\varphi} - 2e^{-\sqrt{\frac{2d_1}{d_1+2}}\,\varphi}\right]\,. \tag{B.1}$$

Exact expressions for $U(\phi)$ (3.7) and (4.2) indicate that the ratio

$$\frac{U(\phi)}{U(\phi_{min})} = F(\phi,k,d_1) \tag{B.2}$$

depends only on ϕ, k and d_1. Dimensionless parameter $k = \xi\Lambda_D$ for the quadratic model and $k = \gamma\Lambda_D^3$ for the quartic model. In Eq. (B.2) we take into account that ϕ_{min} is a function of k and d_1: $\phi_{min} = \phi_{min}(k,d_1)$. Then, $U(\phi_{min})$ defined in Eqs. (3.7) and (4.2) reads:

$$U(\phi_{min}) = \Lambda_D\tilde{F}(\phi_{min}(k,d_1),k,d_1)\,. \tag{B.3}$$

Therefore, parameters k and d_1 determine fully the shape of the effective potential, and parameter Λ_D serves for conformal transformation of this shape. This conclusion is confirmed also in sections 3 and 4 where we show that positions of all extrema depend only on k and d_1. Thus, figures 2, and 7 for contour plots are defined by k and d_1 and will not change with Λ_D. From the definition of the slow roll parameters it is clear that they also do not depend on the hight of potentials and in our model depend only on k and d_1 (see figures 8 and 9). Similar dependence takes place for difference $\Delta\phi = \phi_{max} - \phi_{min}$ drawn in Fig. 13. Thus the conclusions concerning

the slow roll and topological inflations are fully determined by the choice of k and d_1 and do not depend on the hight of the effective potential, in other words, on Λ_D. So, for fixed k and d_1 parameter Λ_D can be arbitrary. For example, we can take Λ_D in such a way that the hight of the saddle point $\chi_{2(+)}$ will correspond to the restriction on the slow roll inflation potential (see e.g. [41]) $U_{eff} \lesssim 2.2 \times 10^{-11} M_{Pl}^4$, or in our notations $U_{eff} \lesssim 5.5 \times 10^{-10} M_{Pl}^2$.

Above, we indicate figures which (for given k and d_1) do not depend on the hight of the effective potential (on Λ_D). What will happen with dynamical characteristics drawn in figures 10, 11 and 12 (and analogous ones for the quadratic model) if we, keeping fixed k and d_1, will change Λ_D? In other words, we keep the positions of the extrema points (in (φ, ϕ)-plane) but change the hight of extrema. We can easily answer this question using the self-similarity condition of the Friedmann equations. Let the potential U in Eqs. (A.2) and (A.3) be transformed conformally: $U \to c\,U$ where c is a constant. Next, we can introduce a new time variable $\tau := \sqrt{c}\,t$. Then, from Eqs. (A.2)-(A.5) follows that the Friedmann equations have the same form as for the model with potential U where time t is replaced by time τ. This condition we call the self-similarity. Thus, if in our model we change the parameter Λ_D : $\Lambda_D \to c\,\Lambda_D$, it results (for fixed k and d_1) in rescaling of all dynamical graphics (e.g. Figures 10 - 12) along the time axis in $1/\sqrt{c}$ times (the decrease of Λ_D leads to the stretch of these figures along the time axis and vice versa the increase of Λ_D results in the shrink of these graphics). Numerical calculations confirm this conclusion. The property of the conformal transformation of the shape of U_{eff} with change of Λ_D for fixed k and d_1 can be also called as the self-similarity.

[1] H.V.Peiris et al., Astrophys.J.Suppl. 148 (2003) 213, arXiv:astro-ph/0302225.

[2] M. Rainer and A. Zhuk, Gen.Rel.Grav. 32 (2000) 79, arXiv:gr-qc/9808073.

[3] U. Günther and A. Zhuk, Phys. Rev. D56 (1997) 6391, arXiv:gr-qc/9706050v2.

[4] R. Kallosh, N. Sivanandam and M. Soroush, Phys. Rev. D 77 (2008) 043501, arXiv:0710.3429.

[5] A. Linde and A, Westphal, JCAP 0803 (2008) 005, arXiv:0712.1610.

[6] J. P. Conlon, R. Kallosh, A. Linde and F. Quevedo, *Volume Modulus Inflation and the Gravitino Mass Problem*, arXiv:0806.0809.

[7] U. Günther and A. Zhuk, Phys. Rev. D61 (2000) 124001, arXiv:hep-ph/0002009.

[8] T. P. Sotiriou and V. Faraoni, *f(R) Theories Of Gravity*, arXiv:0805.1726.

[9] R. P. Woodard, Lect. Notes Phys., 720 (2007) 403, arXiv:gr-qc/0602110.

[10] S. Nojiri, S. D. Odintsov, *Dark energy, inflation and dark matter from modified F(R) gravity*, arXiv:0807.0685.

[11] U. Günther, A. Zhuk, V.B. Bezerra and C. Romero, Class. Quant. Grav. 22 (2005) 3135, arXiv:hep-th/0409112.

[12] A.A. Starobinsky, Phys. Lett. B91 (1980) 99.

[13] U. Günther, P. Moniz and A. Zhuk, Phys. Rev. D66 (2002) 044014, arXiv:hep-th/0205148.

[14] K.A. Bronnikov and S.G. Rubin, *Abilities of multidimensional gravity*, Grav and Cosmol. Vol.13, No.4 (2007) 253, arXiv:0712.0888.

[15] J. Ellis, N. Kaloper, K. A. Olive and J. Yokoyama, Phys.Rev. D59 (1999) 103503, arXiv:hep-ph/9807482.

[16] A. Linde, Phys.Lett. B327 (1994) 208, arXiv:astro-ph/9402031

[17] T. Appelquist, H.-C. Cheng and B. A. Dobrescu, Phys.Rev. D64 (2001) 035002, arXiv:hep-ph/0012100; E. Ponton and E. Poppitz, JHEP 0106 (2001) 019, arXiv:hep-ph/0105021; H.-C. Cheng, K. T. Matchev and M. Schmaltz, Phys.Rev. D66 (2002) 036005, arXiv:hep-ph/0204342; G. Servant and T. M.P. Tait, Nucl.Phys. B650 (2003) 391, arXiv:hep-ph/0206071; L. Bergstrom, T. Bringmann, M. Eriksson and M. Gustafsson, Phys.Rev.Lett. 94 (2005) 131301, arXiv:astro-ph/0410359; F. De Fazio, *Constraining Universal Extra Dimensions through B decays*, arXiv:hep-ph/0609134.

[18] P.K. Townsend, *Four lectures on M-theory*, arXiv:hep-th/9612121; J.W. Moffat, *M-theory on a supermanifold*, arXiv:hep-th/0111225.

[19] A. Kundu, *Universal Extra Dimension*, arXiv:0806.3815.

[20] P.G.O. Freund and M.A. Rubin, Phys. Lett. B97 (1980) 233.

[21] U. Günther, P. Moniz and A. Zhuk, Phys. Rev. D68 (2003) 044010, arXiv:hep-th/0303023 .

[22] A. Zhuk, *Conventional cosmology from multidimensional models*, Proceedings of the 14th International Seminar on High Energy Physics "QUARKS-2006" in St. Petersburg, May 19-25 2006, vol.2, p.264, INR press, 2007, arXiv:hep-th/0609126.

[23] B.Ratra and P.J. Peebles, Phys. Rev. D37 (1988) 3406.

[24] G.F.R. Ellis and M.S. Madsen, Class. Quant. Grav. 8 (1991) 667, .

[25] B. Ratra, Phys. Rev. D45 (1992) 1913.

[26] C. Stornaiolo, Phys. Let.A 189 (1994) 351.

[27] N. Sakai, H. Shinkai, T. Tachizawa and K. Maeda, Phys.Rev. D53 (1996) 655; Erratum-ibid. D54 (1996) 2981, arXiv:gr-qc/9506068.

[28] T. Saidov and A. Zhuk, Phys. Rev. D75 (2007) 084037, arXiv:hep-th/0612217.

[29] N. Arkani-Hamed, S. Dimopoulos, J. March-Russell, Phys.Rev. D63 (2001) 064020, arXiv:hep-th/9809124v2.

[30] U. Günther, A. Starobinsky and A. Zhuk, Phys. Rev. D69 (2004) 044003, arXiv:hep-ph/0306191 .

[31] Y. M. Cho and Y. Y. Keum, Class. Quant. Grav. 15 (1998) 907.

[32] Y. M. Cho and J. H. Kim, *Dilaton as a Dark Matter Candidate and its Detection*, arXiv:0711.2858.

[33] J. Martin, D. Schwarz, Phys.Rev. D62 (2000) 103520, arXiv:astro-ph/9911225.

[34] N. Deruelle, M. Sasaki and Y. Sendouda, *"Detuned" f(R) gravity and dark energy*, arXiv:0803.2742.

[35] T.T. Nakamura and E.D. Stewart, Phys. Lett. B

381 (1996) 413, arXiv:astro-ph/9604103; J.-O. Gong and E.D. Stewart, Phys. Lett. B 538 (2002) 213, arXiv:astro-ph/0202098.
[36] R. Kallosh and S. Prokushkin, *SuperCosmology*, arXiv:hep-th/0403060.
[37] D.H. Lyth and A. Riotto, Phys.Rept. 314 (1999) 1, arXiv:hep-ph/9807278; G. Efstathiou, K.J. Mack, JCAP 0505 (2005) 008, arXiv:astro-ph/0503360.
[38] H. V. Peiris and R. Easther, *Primordial Black Holes, Eternal Inflation, and the Inflationary Parameter Space after WMAP5*, arXiv:0805.2154.
[39] T. Saidov and A. Zhuk, Gravitation & Cosmology, 12 (2006) 253, arXiv:hep-th/0604131.
[40] Alexander Vilenkin, Phys.Rev.Lett. 72 (1994), arXiv:hep-th/9402085.
[41] D.H. Lyth, Phys.Lett. B147 (1984) 403.
[42] A.R. Liddle and D. H. Lyth, Phys.Rept. 231 (1993) 1, arXiv:astro-ph/9303019.
[43] G. Barenboim and O. Vives, About a (standard model) universe dominated by the right matter, arXiv:0806.4389.